

PAPER

Training-induced cortical representation of a hemianopic hemifield

L Henriksson, A Raninen, R Näsänen, L Hyvärinen, S Vanni



More information is available online at <http://www.jnnp.bmjournals.com/supplemental>

See end of article for authors' affiliations

Correspondence to:
L Henriksson, Low Temperature Laboratory, Brain Research Unit, Helsinki University of Technology, PO Box 3000, Espoo 02015 HUT, Finland; henriksson@neuro.hut.fi

Received 5 June 2006
Revised 4 September 2006
Accepted 4 September 2006
Published Online First 15 September 2006

J Neurol Neurosurg Psychiatry 2007;**78**:74–81. doi: 10.1136/jnnp.2006.099374

Background: Patients with homonymous hemianopia often have some residual sensitivity for visual stimuli in their blind hemifield. Previous imaging studies suggest an important role for extrastriate cortical areas in such residual vision, but results of training to improve vision in patients with hemianopia are conflicting.

Objective: To show that intensive training with flicker stimulation in the chronic stage of stroke can reorganise visual cortices of an adult patient.

Methods: A 61-year-old patient with homonymous hemianopia was trained with flicker stimulation, starting 22 months after stroke. Changes in functioning during training were documented with magnetoencephalography, and the cortical organisation after training was examined with functional magnetic resonance imaging (fMRI).

Results: Both imaging methods showed that, after training, visual information from both hemifields was processed mainly in the intact hemisphere. The fMRI mapping results showed the representations of both the blind and the normal hemifield in the same set of cortical areas in the intact hemisphere, more specifically in the visual motion-sensitive area V5, in a region around the superior temporal sulcus and in retinotopic visual areas V1 (primary visual cortex), V2, V3 and V3a.

Conclusions: Intensive training of a blind hemifield can induce cortical reorganisation in an adult patient, and this case shows an ipsilateral representation of the trained visual hemifield in several cortical areas, including the primary visual cortex.

Homonymous hemianopia refers to blindness of a visual hemifield, a common symptom after a lesion in the occipital cortex or in the retinocortical pathway behind the optical chiasm. Neuroimaging studies have indicated residual responsiveness to blind hemifield stimulation in the extrastriate^{1–6} and spared calcarine cortex,⁷ but studies on improvements of residual vision using training have reported conflicting results. Training of visual functions is not a standard procedure after a local cerebral damage, whereas benefits of motor rehabilitation and reorganisation of the motor cortex are widely accepted.⁸ Plasticity in the primary visual cortex (V1) has been described in primate studies,⁹ but there is an ongoing debate on the capacity of adult V1 for major long-term reorganisation.^{10–11} Overall, there is no previous report on a patient whose hemianopia had been intensively trained and the cortical effects of this training studied with functional imaging.

This report describes cortical reorganisation of an adult male patient with homonymous hemianopia. His visual functions in the blind hemifield were trained using difficult detection tasks of flickering discs and recognition of flickering letters. The training procedure and follow-up findings of psychophysical and neuro-magnetic results for this and another patient are described in detail by Raninen *et al.*¹² Spontaneous recovery during training in this patient was unlikely, because training began in the chronic stage of the stroke. We were careful not to let eye movements or stable eccentric fixation contaminate the results.

METHODS

Patient

The patient (IT) was a 61-year-old man who developed homonymous hemianopia after cerebral infarction. The lesion

covered medial parts of the left occipital lobe, involved the calcarine cortex and extended anteriorly towards the left ventricle. Training started 22 months after the stroke, in December 2002. Training was intensive, taking place on average twice a week. After 5 months, flicker detection and sensitivity to recognise flickering letters in the blind hemifield were already comparable to the sensitivity of the normal hemifield.¹² During the follow-up period, he received no drugs affecting the central nervous system.

We followed the effect of training with fully non-invasive magnetoencephalography (MEG), and proceeded to map the cortical reorganisation with functional magnetic resonance imaging (fMRI). IT participated altogether in 13 MEG and 8 fMRI/MRI measurement sessions. Here, we show MEG results from measurements before (November 2002) and after 2 years of training (November 2004), and results from fMRI/MRI sessions measured as follows: anatomical images in September 2003, location of V5 in February 2004, MEG stimulus in fMRI in November 2004, phase-encoded retinotopic mapping in January 2005 and multifocal fMRI in April 2005. The training continued along with the fMRI measurements.

In addition, two of the authors (LH and SV) participated in a control experiment where we mapped changes in multifocal fMRI results during voluntary eccentric fixation and saccadic eye movements (details are available online at <http://www.jnnp.bmjournals.com/supplemental>).

Abbreviations: fMRI, functional magnetic resonance imaging; MCE, minimum current estimate; MEG, magnetoencephalography

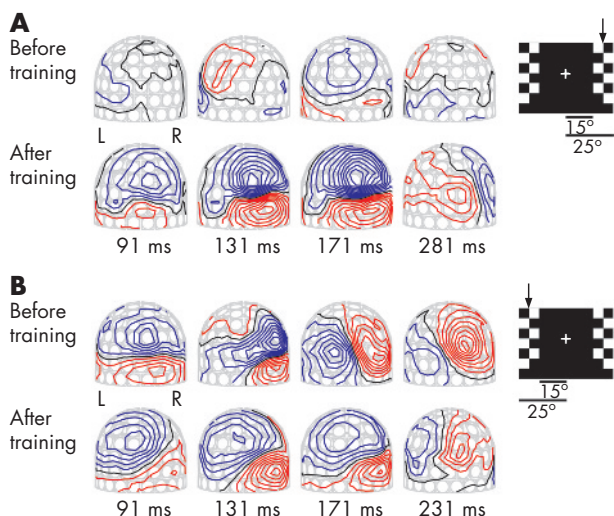


Figure 1 Magnetic field patterns evoked by pattern-reversal checkerboard stimulation before and after 2 years of training. The insert shows one frame of the stimulus, with the stimulated hemifield indicated with an arrow. The checkerboard pattern reversed in the left or right hemifield in random order. The MEG helmet is viewed from the back, response latency is indicated in ms and the field contour step is 20 fT. (A) MEG field patterns during stimulation of the blind (right) hemifield. Stimulation evoked no measurable MEG response before the onset of the training. (B) The field patterns during stimulation of the normal hemifield. L, left hemisphere; R, right hemisphere.

Stimuli

The stimulus in MEG consisted of two 10°-wide and 35°-high checkerboard patterns on both sides of the fixation, starting at 15° eccentricity. MEG responses were measured for contrast reversals of checkerboards on either side of the fixation. Interstimulus interval was 0.9–1.1 s between the contrast reversals, randomised between the hemifields. The total interstimulus interval within a hemifield varied from 0.9 to 10.0 s. The only difference in the checkerboard stimulus in fMRI was that hemifields had to be stimulated in different runs because the narrow magnet bore and head coil limited the horizontal visual field to about 26° in diameter. The fMRI series comprised four 6-min runs/hemifield. Phase-encoded retinotopic mapping with rotating wedge-shaped stimulus disclosed cortical representation of the meridional positions (polar angle) in the normal hemifield to 25° eccentricity.^{13, 14} The checkerboard pattern within the wedge reversed contrast at 8 Hz. The location of the motion-sensitive visual area V5 was mapped with a low-contrast (10%) concentric expanding and contracting (7°/s) stimulus. IT's ability to fixate was controlled with a multifocal stimulus,¹⁵ where the normal hemifield was divided into 30 regions from 0.5° to 12° radius, and stimulated in parallel with one visual field segment from 6° to 12° radius in the blind hemifield. Within the stimulated regions, the checkerboard pattern reversed contrast at 8 Hz.

Stimuli were created with Matlab (Mathworks, Natick, MA, USA) and the timing was controlled with Presentation (Neurobehavioral Systems, Albany, CA, USA). Stimuli were presented via three-micromirror data projectors (in MEG Vista Project, Electrohome, Kitchener, Ontario, Canada, and in fMRI Christie X3TM, Christie Digital Systems, Kitchener, Ontario, Canada) and back-projection systems.

Data acquisition and analysis

MEG measurements were performed using a whole-head 306-channel Vectorview neuromagnetometer (Elekta-Neuromag,

Stockholm, Sweden). During MEG measurements, the eye movements were recorded with horizontal and vertical electro-oculograms. Epochs with blinks or saccades were rejected online with a rejection threshold of 150 μ V. In the last two measurements, stable eccentric fixation was ruled out by observing IT's eye position via a mirror. Stable eye position error more than approximately 2° was detectable. The MEG data were band pass filtered (0.1–200 Hz), sampled (600 Hz) and averaged time locked to the stimulus. Time–frequency representations were calculated with a wavelet-based method using 4D Toolbox (provided by Ole Jensen, FC Donders Centre for Cognitive Neuroimaging, Nijmegen, The Netherlands). Minimum current estimate (MCE) analysis with the individual boundary element model was applied to the MEG data.¹⁶ MCE is an application of the minimum L1-norm estimate.¹⁷ Region of interests were selected to enclose major activation and to show corresponding dynamics.

fMRI measurements were performed using a 3-T Signa MRI scanner (General Electric, Milwaukee, Wisconsin, USA). A high-resolution anatomical MRI scan optimised for segmentation of grey and white matter was acquired with spoiled gradient-echo sequence. The acquisition parameters were field of view (FOV) 23 cm, imaging matrix 256×256, slice thickness 0.9 mm and number of slices ($n = 124$). Single-shot gradient-echo echo-planar imaging was used in all functional series. The location of area V5 was mapped with imaging parameters repetition time (TR) 1.999 s, FOV 19 cm, imaging matrix 64×64, slice thickness 3 mm and $n = 27$. The same imaging parameters were used when the MEG stimulus was adapted for fMRI. In the phase-encoded mapping of retinotopy, imaging parameters were TR 1.239 s, FOV 20 cm, imaging matrix 64×64, slice thickness 4 mm and $n = 16$. In every fMRI session, a low-resolution structural MRI scan was acquired to coregister functional series with the high-resolution MRI. Eye movements were observed during pattern-reversal stimulations with a camera, and losses of fixation greater than approximately 5° were detectable. In multifocal fMRI, the imaging parameters were TR 1.819 s, FOV 16 cm, imaging matrix 64×64, slice thickness 2.5 mm and $n = 24$.

fMRI data were analysed with standard preprocessing and statistical methods using the SPM2 (Wellcome Department of Imaging Neuroscience, London, UK) Matlab toolbox. The Brain à la Carte toolbox, Grenoble, France was used for surface-oriented analysis.¹⁴

RESULTS

Figure 1 shows the change in the MEG field patterns during training. Before training, stimulation of the blind hemifield evoked no measurable responses. The responses appeared over the right hemisphere and increased to reach the same amplitude as responses after stimulation of the normal hemifield.¹² In the recording after 2 years of training, there were robust field patterns for the stimulation of the blind (right) hemifield over the right hemisphere, emerging over the medial occipital regions and then moving to more temporal regions (fig 1A). Figure 1B shows the MEG field patterns after stimulation of the normal hemifield. These evoked fields were clearly affected during the training of the blind hemifield.

As ipsilateral visual processing is exceptional, we examined the reactivity of spontaneous oscillations for further support. Typically, spontaneous oscillations close to sensory cortices attenuate transiently after sensory stimulation.¹⁸ Figure 2 shows time–frequency representations of oscillatory activity time locked to stimulation of the blind hemifield, averaged over a set of channels over the occipital lobes. Before training, left-side channels showed strong oscillations in the frequency range of 8–13 Hz with minor reactivity to stimulation (fig 2A), whereas the

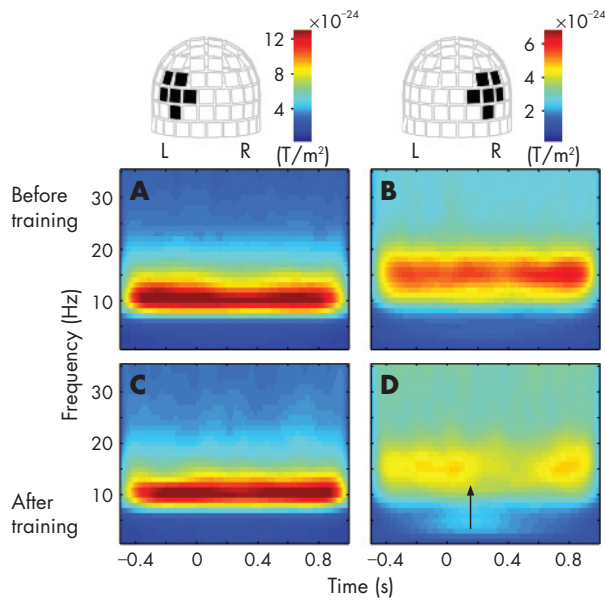


Figure 2 Averaged time–frequency representations of the oscillatory activity for stimulation of the blind hemifield before and after training. On the top, the helmet-shaped measurement array is viewed from the back, and the black rectangles indicate the averaged channels. Change in the head position between the two measurements is negligible, enabling direct comparison of the datasets. The upper panels show the mean power of the left (A) and right (B) hemisphere before training and the lower panels (C,D) after training. Arrow at 150 ms indicates the onset of suppression. L, left hemisphere; R, right hemisphere.

channels over the right occipital lobe showed the strongest oscillations in the frequency range of 13–17 Hz without any reactivity (fig 2B). After 2 years of training, the oscillations showed almost no suppression on the left side (fig 2C), but oscillatory activity on the right side was clearly suppressed at 150 ms after stimulus presentation (fig 2D, arrow). Strong oscillations may hide minor reactivity on the left, but obviously, training has mainly affected the behaviour of the intact (right) hemisphere. While the right occipital lobe has gained reactivity for stimulation of the blind (right) hemifield, the strong non-reactive oscillations on the left suggested functional disconnection of the left occipital cortex from visual input.

To identify major source regions and their dynamics, MCE analysis was applied to the MEG data acquired after training. Figure 3A shows the mean estimated brain activity between 100 and 200 ms after stimulations of the blind and normal hemifields. The MCEs show single maxima, which can be explained with active brain areas shown with ellipsoids over the magnetic resonance image. The activity is presumably emerging from several visual areas. The mean location of the source after stimulation of the blind hemifield is in the same hemisphere but located more posteriorly than the source activated by stimulation of the normal hemifield. Time courses of the selected regions of interest show how the response after stimulation of the blind hemifield peaks later than the steep response after stimulation of the normal hemifield. Figure 3B shows MCEs between 275 and 320 ms after stimulation of the blind hemifield and between 160 and 180 ms after stimulation of the normal hemifield. The lateral activities can be localised close to the visual motion-sensitive area V5. Compared with the normal hemifield, the V5 activation is delayed after stimulation of the blind hemifield stimulation.

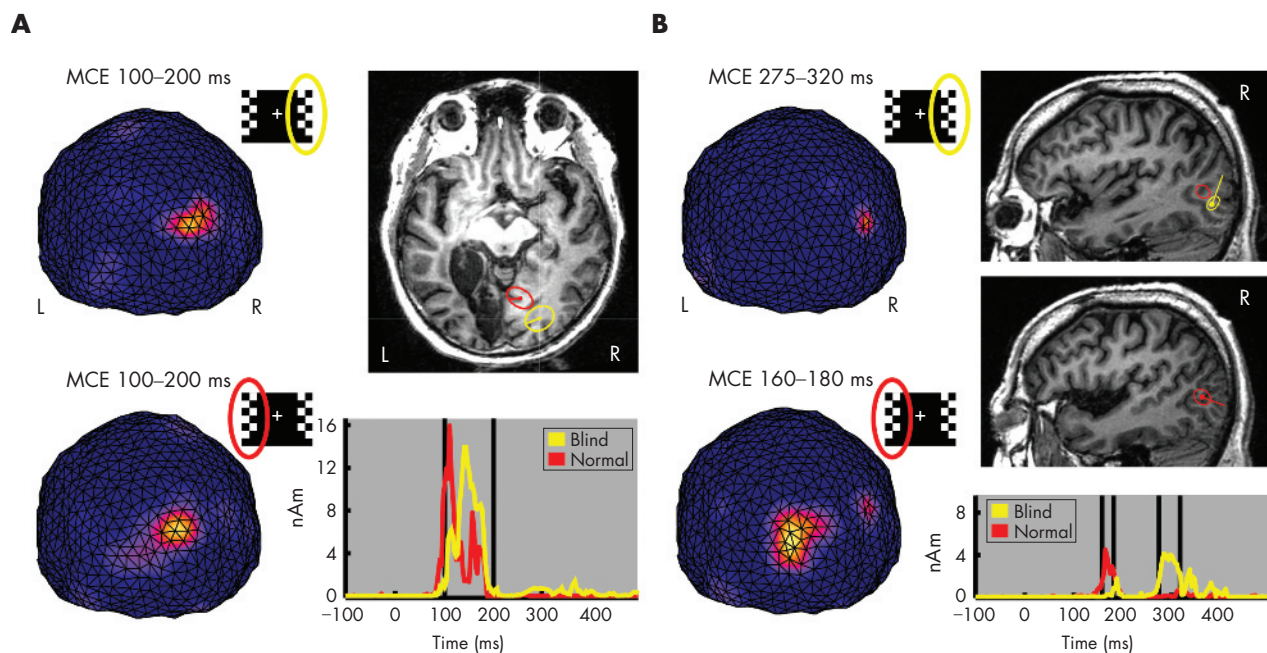


Figure 3 Minimum current estimates (MCEs), mean locations of sources, and time courses of the sources after training. (A) MCEs between 100 and 200 ms viewed from the back (L, left hemisphere; R, right hemisphere). Source explaining the response evoked by stimulation of the blind hemifield is shown in yellow and that by stimulation of the normal hemifield in red. The radii of the reported regions of interest (ROIs; ellipsoids on the magnetic resonance images (MRIs), the line indicating the current direction) show the distances at which the weighting functions are reduced to 60%. Vertical lines indicate the time range 100–200 ms. (B) MCEs between 275 and 320 ms after stimulation of the blind hemifield and between 160 and 180 ms after stimulation of the normal hemifield, and the locations of sources (R, right sagittal slice) and time courses of sources. nAm, nanoampere-meter.

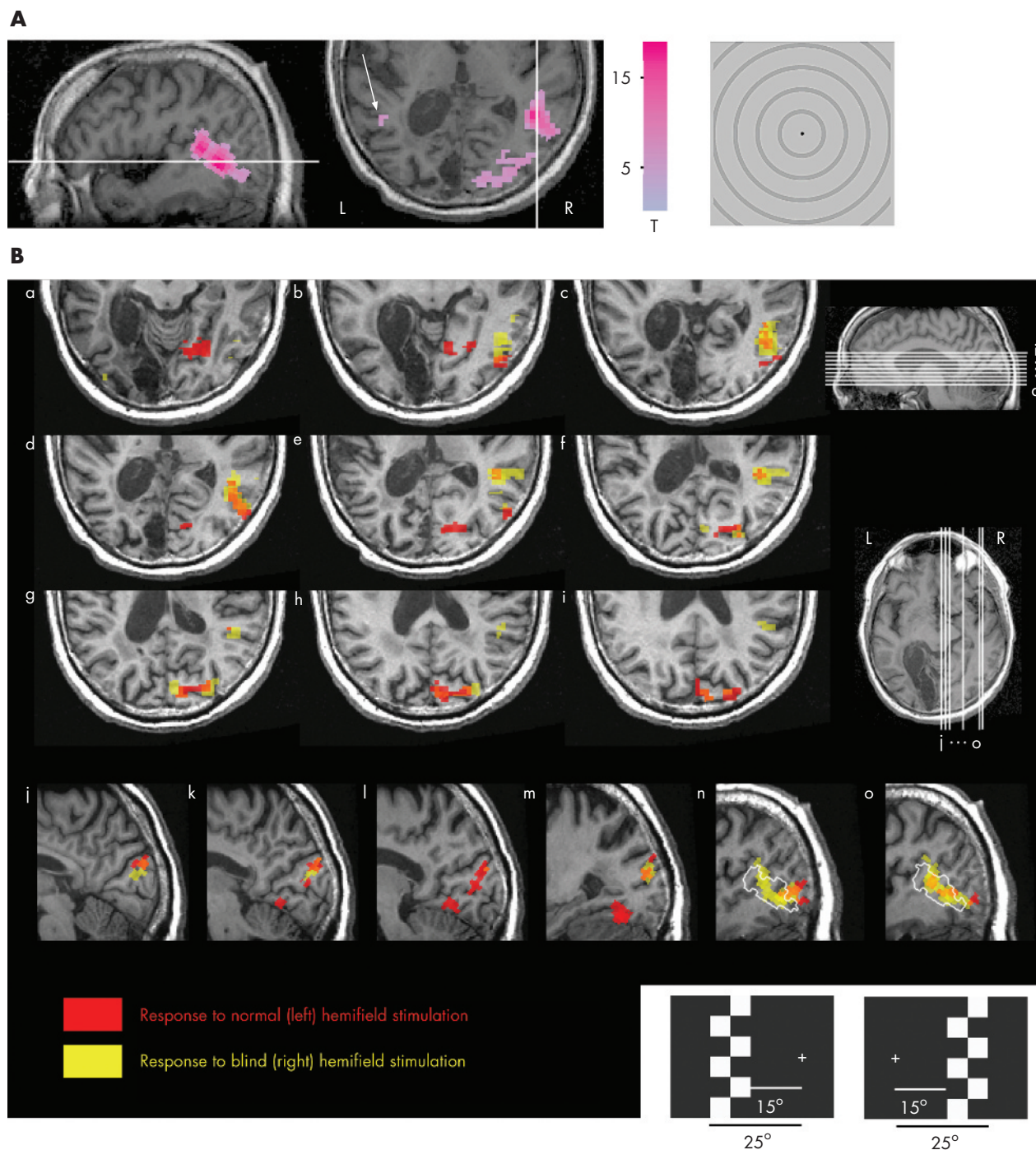


Figure 4 Functional magnetic resonance imaging (fMRI) activations for motion and pattern-reversal stimulations after training. (A) fMRI statistical parametric mapping (SPM (t)) for whole-field radial contracting and expanding motion stimulus is thresholded at family-wise-error-corrected p Value (p_{FWE}) < 0.05 and overlaid on patient’s structural MRI (L, left hemisphere; R, right hemisphere). The white lines indicate the section of the other orientation. The arrow points to the minor activation in the lesioned (left) hemisphere. (B) Activation SPM(t) map (thresholded at p_{FWE} < 0.05) for the pattern-reversal stimulation of the normal (left) hemifield pattern is shown in red and that for stimulation of the blind (right) hemifield in yellow. Nine axial slices (a–i) and six sagittal slices (j–o) are shown. The white contour in slices n and o indicates the borders of the mapped V5 and the satellite area around the superior temporal sulcus.

In fMRI, we first localised the visual motion-sensitive area V5 with a low-contrast circularly symmetrical moving stimulus, and found a strong asymmetry between the hemispheres (fig 4A). In the intact hemisphere, V5 and a more dorsal and anterior satellite area around the superior temporal sulcus were strongly activated, whereas in the lesioned hemisphere only a

marginal response was visible around a typical V5 location (arrow). To explore the functional reorganisation after training, the pattern-reversal checkerboard stimulus evoking clear signals in MEG (fig 1) was transferred to fMRI. Figure 4B shows activations for both the stimulation of the normal and blind hemifields. Consistent with the MEG field patterns,

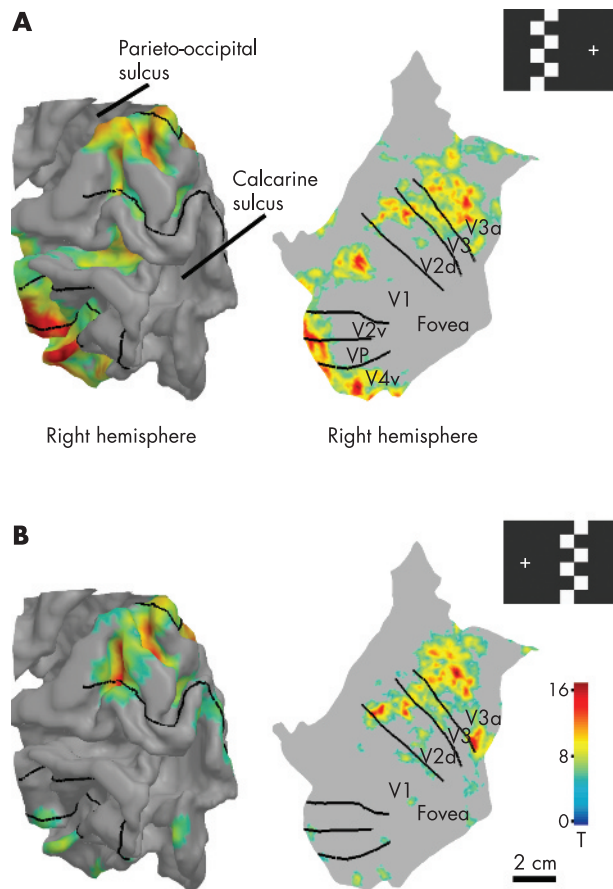


Figure 5 Representations of the blind and normal hemifields in low-order retinotopic areas shown on a segmented and reconstructed model of the right occipital lobe. (A) Pattern-reversal checkerboard stimulation of the left hemifield activates retinotopic visual areas as expected according to stimulus position. Borders between retinotopic areas were mapped with phase-encoded retinotopic mapping. (B) Stimulated region in the blind (right) hemifield is represented in the same visual areas with the normal hemifield in the intact (right) occipital cortex, extending mainly to the visual areas dorsal of the calcarine sulcus.

during stimulation of either of the hemifields, fMRI activations were in the posterior right hemisphere, including medial and lateral occipital and superior temporal regions. The lateral activation cluster overlaps the location of the response to visual motion, showing that the motion-sensitive area V5 and the region around the superior temporal sulcus were sensitive to both low-contrast motion and pattern reversal.

To examine more closely the visual field representation in the retinotopic visual areas, the fMRI responses for the checkerboard stimulations were assigned to IT's segmented and reconstructed cortical surface of the intact occipital lobe (fig 5). The borders between retinotopic visual areas were localised with mapping of the meridional position (polar angle) in the normal hemifield using a rotating wedge-shaped stimulus.^{13–14} In retinotopic areas, eccentricity is coded as distance from the representation of the central visual field near the occipital pole (foveal confluence). Activation during the checkerboard stimulation of the normal hemifield extends to all these retinotopic areas, and is located as presumed based on the stimulus starting 15° off the vertical meridian. Stimulation of the corresponding region in the blind hemifield activated mainly dorsal occipital areas in the intact hemisphere,

especially V3a, but also V3, dorsal V2 (V2d) and a border region between V1 and V2d.

The stability of the fixation and the bilateral visual field representation in the retinotopic areas were verified with a multifocal fMRI experiment.¹⁵ With this method, responses from multiple visual field positions were mapped simultaneously using parallel but temporally orthogonal stimulation sequences. Figure 6A shows an example frame of a multifocal stimulus with 30 regions in the left and one region in the right hemifield. During one frame, half of the regions are on and the other half off, and the set of active regions changes every 10.9 s. In fig 6B the activation for stimulation of the blind hemifield is assigned to IT's reconstructed and unfolded cortical surface of the intact (right) occipital lobe. In addition, V5 and the dorsal satellite region in both hemispheres were active for this stimulation (data not shown). This was the last measurement, and the first time we recorded good signals from IT's V5 in the left hemisphere. Bilateral activity in V5 without responsiveness of early visual cortical areas has been reported previously.⁴ We assume that continuing training was changing the functional organisation even after >2 years of training. Figure 6C shows the normal retinotopic organisation of responses as a function of eccentricity mapped with multifocal stimulation of the normal (left) hemifield. The unfolded view shows overlapping representations of the hemifields (arrow). Figure 6D confirms the accuracy between the retinotopic maps obtained with the multifocal method and the phase-encoded approach. The polar angle map of the normal hemifield (multifocal data) and the borders between retinotopic areas (phase-encoded data) are in register as expected (see online material available at <http://www.jnnpbjournals.com/supplemental>).

DISCUSSION

Training induced functional reorganisation in the intact hemisphere in visual areas V1, V2, V3, V3a and V5, and in the putative human superior temporal polysensory¹⁹ area around the superior temporal sulcus. The representation of the blind hemifield is distributed to the same functionally defined cortical areas with the normal hemifield representation. In accordance with this reorganisation, the fields evoked by stimulation of the normal hemifield appear to have shifted during the training (fig 1). Our results, showing the strongest responsiveness to the stimulation of the blind hemifield in V5, V3a and the superior temporal polysensory area, are in line with studies on macaque monkeys with inactivated primary visual cortex,^{20–22} but extend the previous findings by indicating strong involvement of low-level retinotopic areas. The reorganisation of low-level retinotopic areas could be due to the combination of long rehabilitation, repeated difficult tasks in the training and ipsilateral processing—that is, processing in a healthy part of the brain, where these retinotopic areas are available. Ipsilateral processing of residual vision, including areas V3/V3a and V5, has been shown in patients who have undergone hemispherectomy.^{23–24} In healthy people, much more limited ipsilateral responses are found.²⁵ The probable explanation for why training enhanced ipsilateral instead of contralateral processing of residual vision is the possible partial functional disconnection of the left occipital regions from the visual processing, as suggested by the strong poorly reacting oscillations (fig 2).

Unsteady fixation has been suspected to be the main cause of enlargement of the visual field.²⁶ If a patient is looking, perhaps unconsciously, toward the stimulus in the blind hemifield instead of fixating steadily at the fixation cross, stimulation of the blind hemifield could be seen by the normal hemifield. Here we list five major proofs against fixation inaccuracies in our data.

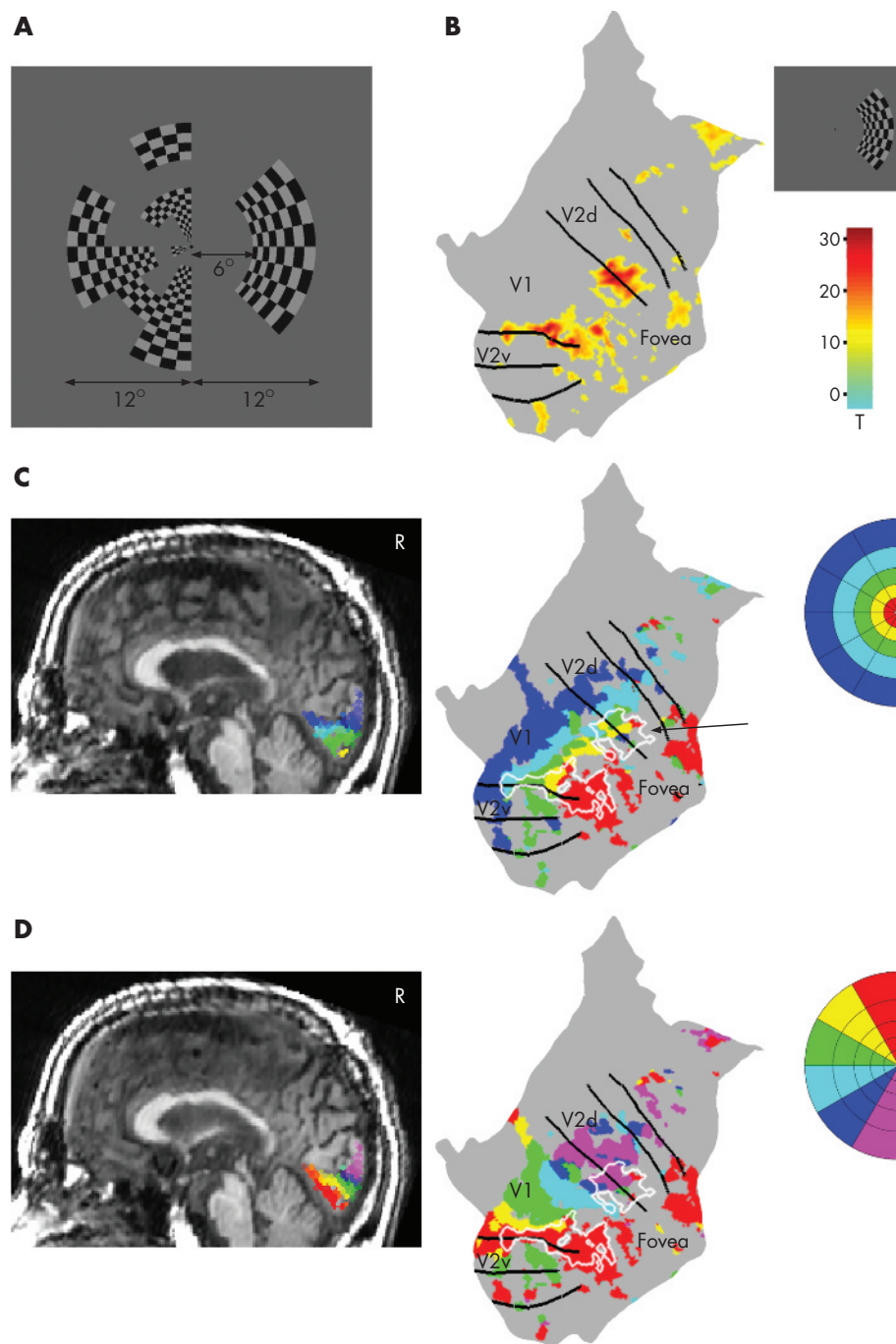


Figure 6 Fixation control measurement with a 31-region multifocal magnetic resonance image (fMRI). (A) An example of a multifocal stimulus frame. The patient fixates on a point in the middle of the display. (B) Response to multifocal stimulation of the blind (right) hemifield assigned to the cortical surface of the patient's intact (right) occipital cortex. The black lines indicate the borders between retinotopic areas. (C) Responses to multifocal stimulation of the normal (left) hemifield shown on his structural magnetic resonance image (activations thresholded at $p_{FWE} < 0.05$, R; right sagittal slice) and assigned to the cortical surface of the intact occipital cortex (thresholded at $T > 10$). Colours of the activated clusters code the eccentricity of the visual field. In the unfolded view, the white outline indicates the location of the response to multifocal stimulation of the blind hemifield. (D) Same data as in (C), but colours code the polar angle of the normal hemifield, enabling the comparison between retinotopic organisations mapped with the multifocal method and borders between retinotopic areas mapped with the phase-encoded approach.

- Consistent results in follow-up imaging data and successful training are found independently in MEG and psychophysical¹² experiments, where several different control measures for eye position were used.
- Our patient was experienced. In the few fMRI sessions where fixation was unstable, activation in the retinotopic areas was strongly attenuated (two sessions before video control, data not shown). Experienced subjects, on average, move their eyes only about 10 arcmin,²⁷ and patients with homonymous hemianopia keep their fixation comparable before and after training of visual functions.²⁸
- In some experiments, the eye position was followed online on a video display, and fixation instabilities exceeding the proximal edge of the peripheral stimulus would have been detected.
- In fig 5, the activations in response to stimulations of the right and left hemifield in the right V2d, V3 and V3a are at approximately the same distance from the foveal confluence. If activation during stimulation of the blind hemifield was derived from eccentric fixation, the patient should have fixated far outside the display on the right, instead of fixation cross on the left.

- IT's ability to fixate was controlled with multifocal fMRI,¹⁵ where regions in the visual field are stimulated in parallel.

If the subject cannot keep fixation, retinotopy breaks down (no signals emerge); and if the subject has stable eccentric fixation, retinotopy shows unusual organisation of the responses. Figure 6 shows the retinotopic map of responses during multifocal stimulation of the normal (left) hemifield. The activation is strongest in the primary visual cortex and extends to neighbouring retinotopic areas, which is a typical distribution of responses expected for a normal visual field in a multifocal fMRI experiment.¹⁵ If IT had had stable eccentric fixation on the right side of the fixation point, the activation coded in colour in fig 6C should be more distant from the foveal confluence than the activation shown by white lines, and the activation patterns coded in red and purple in fig 6D should be inside V1 and not at the border between visual areas V1 and V2, where the vertical meridian is represented (more details are available online at <http://jnnpbjournals.com/supplemental>).

Owing to parallel stimulation of the hemifields, findings from the multifocal data can only be explained by activation of retinotopic areas of the intact hemisphere by stimuli in either hemifield.

During training, IT became conscious of his right hemifield, patches of form vision emerged, and the far periphery of the blind hemifield brightened. Restored function and the coinciding right hemisphere activation are due to therapeutic intervention, and not to spontaneous recovery. Spontaneous recovery occurs typically within the first 3 months after unilateral visual field loss,²⁹ although single cases have continued improving without treatment for up to 2 years.^{30–31} In our patient, training was performed in the third and fourth year after the stroke. Before, IT showed a stable homonymous hemianopia, with no evoked neuromagnetic responses in response to the stimulation of his blind hemifield. At such a chronic stage after brain injury, the probability of any further spontaneous recovery is negligible, and restoration of function must result from intervention.^{32–33}

Callosal connections have been proposed to mediate ipsilateral extrastriate activations documented with healthy subjects,²⁵ but the extent of ipsilateral processing differs between IT and healthy people. As only minor activation was detected in IT's left hemisphere (fig 4), callosal connections seem to be an improbable explanation. A subcortical pathway including strengthened interhemispheric commissural connections of the superior colliculus,³⁴ distributing left hemisphere activity to the right extrastriate visual areas via the pulvinar, is a more plausible explanation. The routing from the right hemifield to the right occipital lobe remains unclear, but the dynamics of the processing (fig 3) suggest that stimulation of the affected hemifield would activate the lower-tier areas directly and not through an extrastriate area such as V5.

ACKNOWLEDGEMENTS

We thank J M Hupé and V Virsu for insightful comments on the manuscript, M Kattelus for help with the fMRI measurements, and A Tarkiainen and S Taulu for technical support. The Brain à la Carte toolbox was provided by unite mixte INSERM/Université Joseph Fourier 594, Grenoble, France.

Authors' affiliations

L Henriksson, S Vanni, Advanced Magnetic Imaging Centre and Brain Research Unit of Low Temperature Laboratory, Helsinki University of Technology, Espoo, Finland

A Raninen, Department of Biological and Environmental Sciences, University of Helsinki, Helsinki, Finland

R Näsänen, Brainwork Laboratory, Finnish Institute of Occupational Health, Helsinki, Finland

L Hyvärinen, Faculty of Behavioural Sciences, University of Helsinki, Helsinki, Finland

Funding: This work was supported by the Academy of Finland, Instrumentarium Science Foundation, the Finnish Graduate School of Neuroscience, the Finnish Cultural Foundation, the De blindas vänner rf—Sokeain Ystävät ry and the Finnish Medical Foundation.

Competing interests: None.

Ethical approval: This study was approved by the ethics committees of the Hospital District of Helsinki and Uusimaa. The participant gave written informed consent before the measurements. Tenets of the Declaration of Helsinki were followed.

REFERENCES

- 1 **Piito M**, Johansen P, Faubert J, et al. Activation of human extrageniculostriate pathways after damage to area V1. *NeuroImage* 1999;**9**:97–107.
- 2 **Baseler HA**, Morland AB, Wandell BA. Topographic organization of human visual areas in the absence of input from primary cortex. *J Neurosci* 1999;**19**:2619–27.
- 3 **Rossion B**, de Gelder B, Pourtois G, et al. Early extrastriate activity without primary visual cortex in humans. *Neurosci Lett* 2000;**279**:25–8.
- 4 **Goebel R**, Muckli L, Zanella FE, et al. Sustained extrastriate cortical activation without visual awareness revealed by fMRI studies of hemianopic patients. *Vision Res* 2001;**41**:1459–74.
- 5 **Nelles G**, Widman G, de Greiff A, et al. Brain representation of hemifield stimulation in poststroke visual field defects. *Stroke* 2002;**33**:1286–93.
- 6 **Schoenfeld MA**, Noesselt T, Poggel D, et al. Analysis of pathways mediating preserved vision after striate cortex lesions. *Ann Neurol* 2002;**52**:814–24.
- 7 **Morland AB**, Le S, Carroll E, et al. The role of spared calcarine cortex and lateral occipital cortex in the responses of human hemianopes to visual motion. *J Cogn Neurosci* 2004;**16**:204–18.
- 8 **Calautti C**, Baron JC. Functional neuroimaging studies of motor recovery after stroke in adults: a review. *Stroke* 2003;**34**:1553–66.
- 9 **Gilbert CD**, Wiesel TN. Receptive field dynamics in adult primary visual cortex. *Nature* 1992;**356**:150–2.
- 10 **Smirnakis SM**, Brewer AA, Schmid MC, et al. Lack of long-term cortical reorganization after macaque retinal lesions. *Nature* 2005;**435**:300–7.
- 11 **Calford MB**, Chino YM, Das A, et al. Neuroscience: rewiring the adult brain. *Nature*. 2005;**438**: discussion E3–4).
- 12 **Raninen A**, Vanni S, Hyvärinen L, et al. Temporal sensitivity in hemianopic visual field can be improved by long-term training using flicker stimulation. *J Neural Neurosurg Psychiatry* 2006;**78**:66–73.
- 13 **Sereno MI**, Dale AM, Reppas JB, et al. Borders of multiple visual areas in humans revealed by functional magnetic resonance imaging. *Science* 1995;**268**:889–93.
- 14 **Warming J**, Dojat M, Guerin-Dugue A, et al. fMRI retinotopic mapping—step by step. *NeuroImage* 2002;**17**:1665–83.
- 15 **Vanni S**, Henriksson L, James AC. Multifocal fMRI mapping of visual cortical areas. *NeuroImage* 2005;**27**:95–105.
- 16 **Uutela K**, Hämäläinen M, Somersalo E. Visualization of magnetoencephalographic data using minimum current estimates. *NeuroImage* 1999;**10**:173–80.
- 17 **Matsuura K**, Okabe Y. Selective minimum-norm solution of the biomagnetic inverse problem. *IEEE Trans Biomed Eng* 1995;**42**:608–15.
- 18 **Hari R**, Salmelin R. Human cortical oscillations: a neuromagnetic view through the skull. *Trends Neurosci* 1997;**20**:44–9.
- 19 **Beauchamp MS**, Lee KE, Argall BD, et al. Integration of auditory and visual information about objects in superior temporal sulcus. *Neuron* 2004;**41**:809–23.
- 20 **Bruce CJ**, Desimone R, Gross CG. Both striate cortex and superior colliculus contribute to visual properties of neurons in superior temporal polysensory area of macaque monkey. *J Neurophysiol* 1986;**55**:1057–75.
- 21 **Gross CG**. Contribution of striate cortex and the superior colliculus to visual function in area MT, the superior temporal polysensory area and the inferior temporal cortex. *Neuropsychologia* 1991;**29**:497–515.
- 22 **Bullier J**, Girard P, Salin P-A. The role of area 17 in the transfer of information to extrastriate visual cortex. *Cerebral Cortex* 1994;**10**:301–330.
- 23 **Bittar RG**, Piito M, Faubert J, et al. Activation of the remaining hemisphere following stimulation of the blind hemifield in hemispherectomized subjects. *NeuroImage* 1999;**10**:339–46.
- 24 **Marx E**, Stephan T, Bense S, et al. Motion perception in the ipsilateral visual field of a hemispherectomized patient. *J Neural* 2002;**249**:1303–6.
- 25 **Tootell RB**, Mendola JD, Hadjikhani NK, et al. The representation of the ipsilateral visual field in human cerebral cortex. *Proc Natl Acad Sci USA* 1998;**95**:818–24.
- 26 **Balliet R**, Blood KM, Bach-y-Rita P. Visual field rehabilitation in the cortically blind? *J Neural Neurosurg Psychiatry* 1985;**48**:1113–24.
- 27 **Putnam NM**, Hofer HJ, Doble N, et al. The locus of fixation and the foveal cone mosaic. *J Vis* 2005;**5**:632–9.
- 28 **Kasten E**, Bunzenthall U, Sabel BA. Visual field recovery after vision restoration therapy (VRT) is independent of eye movements: an eye-tracker study. *Behav Brain Res* 2006. In press. Doi:10.1016/j.bbr.2006.07.024.

- 29 Zhang X, Kedar S, Lynn MJ, *et al.* Natural history of homonymous hemianopia. *Neurology* 2006;**66**:901–5.
- 30 Zihl J. *Rehabilitation of visual disorders after brain injury*. Hove: Psychology Press, 2000.
- 31 Poppel DA, Kasten E, Muller-Oehring EM, *et al.* Unusual spontaneous and training induced visual field recovery in a patient with a gunshot lesion. *J Neurol Neurosurg Psychiatry* 2001;**70**:236–9.
- 32 Liepert J, Bauder H, Wolfgang HR, *et al.* Treatment-induced cortical reorganization after stroke in humans. *Stroke* 2000;**31**:1210–16.
- 33 Rossini PM, Calautti C, Pauri F, *et al.* Post-stroke plastic reorganisation in the adult brain. *Lancet Neurol* 2003;**2**:493–502.
- 34 Tardif E, Clarke S. Commissural connections of human superior colliculus. *Neuroscience* 2002;**111**:363–72.

NEUROLOGICAL PICTURE

doi: 10.1136/jnnp.2006.098517

A case of brain embolism during catheter embolisation of head arteriovenous malformation. What is the mechanism of stroke?

A 52-year-old man presented with facial swelling owing to progression of arteriovenous malformation (AVM). Angiography under endotracheal anaesthesia showed the right internal maxillary, right ascending pharyngeal and right superficial temporal arteries feeding an AVM (fig 1A). Clear connections to the intracranial circulation were not found. Vessels were embolised using N-butyl-2-cyanoacrylate and iodinated oily x ray contrast medium comprising 40% iodine in poppy seed oil (Lipiodol; Terumo, Tokyo, Japan; fig 1B).

After AVM embolisation, disturbance of consciousness and left hemiparesis were present. Diffusion-weighted magnetic resonance imaging showed multiple hyperintense lesions of the right middle cerebral artery, right posterior cerebral artery and right posterior inferior cerebellar artery territories (fig 2A). Computed tomography showed low-density lesions with high-density spots (fig 2B). We confirmed a patent foramen ovale (PFO) using transcranial Doppler and transoesophageal echocardiography with saline contrast. No lesions contributing to cerebral embolism were present in the carotid artery or the aortic arch. We finally considered that paradoxical brain embolism occurred because of embolic material passing through the PFO.

Cerebral complications during catheter embolisation have rarely been described in detail.^{1,2} Firstly, embolic material would have had to pass from the artery to the vein through the cerebral AVM during catheter embolisation. Pulmonary embolism as a complication of transcatheter arterial embolisation has indeed been documented.³ Secondly, mechanical ventilation may have contributed to an elevation of right atrial pressure. Increasing pressure in the right atrium would generate conditions such as a Valsalva manoeuvre. Therefore,

embolic material could have passed from the right to the left atrium through the PFO, resulting in multiple brain infarctions.

Y Iguchi, K Kimura

Department of Stroke Medicine, Kawasaki Medical School, Kurashiki-City, Japan

Correspondence to: Y Iguchi, Department of Stroke Medicine, Kawasaki Medical School, 577 Matsushima, Kurashiki-city, Okayama 701-0192, Japan; yigu@med.kawasaki-m.ac.jp

Competing interests: None declared.

References

- 1 Horowitz MB, Carrau R, Crammond D, *et al.* Risks of tumor embolization in the presence of an unrecognized patent foramen ovale: case report. *Am J Neuroradiol* 2002;**23**:982–4.
- 2 Yoo KM, Yoo BG, Kim KS, *et al.* Cerebral lipiodol embolism during transcatheter arterial chemoembolization. *Neurology* 2004;**63**:181–3.
- 3 Kjellin IB, Boechar M, Vinuela F, *et al.* Pulmonary emboli following therapeutic embolization of cerebral arteriovenous malformations in children. *Pediatr Radiol* 2000;**30**:279–83.

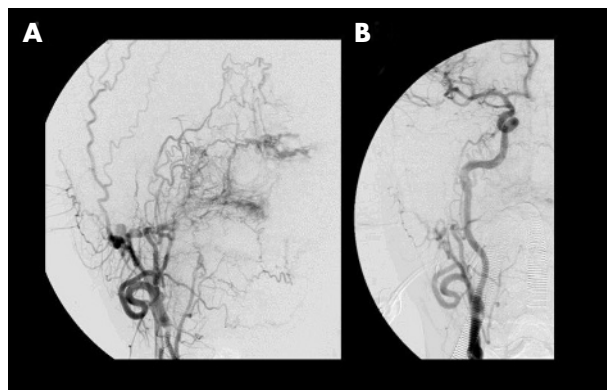


Figure 1 (A) Right external carotid arteriography shows the right internal maxillary, right ascending pharyngeal and right superficial temporal arteries feeding vessels to a cerebral arteriovenous malformation (AVM). (B) Common carotid arteriography shows branches of the external carotid artery feeding vessels to the AVM.

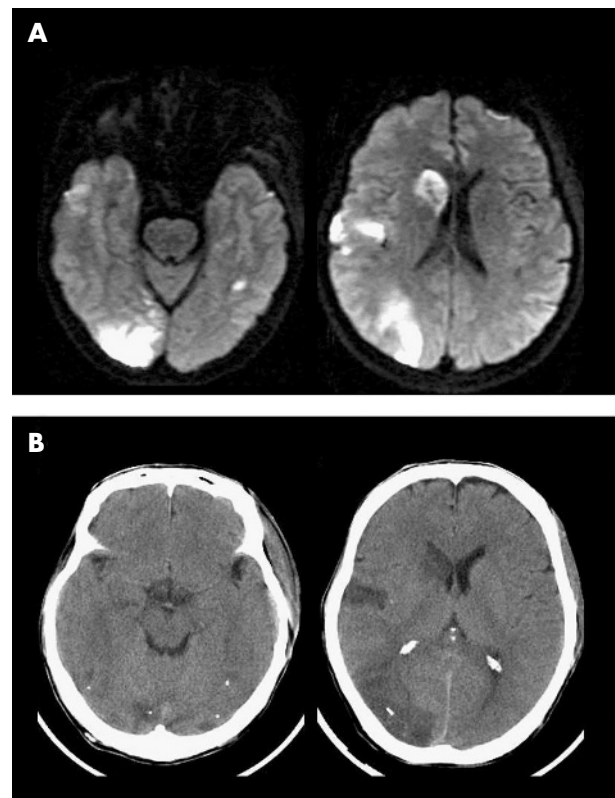


Figure 2 (A) Diffusion-weighted magnetic resonance imaging shows multiple hyperintense lesions in the right occipital and temporal lobes and right caudate nucleus. (B) Computed tomography shows a hypodense lesion in the right occipital lobe. Multiple hyperdense lesions are present in bilateral occipital lobes, showing evidence of embolic material.